

A Notched Disk Crack Propagation Test for Asphalt Concrete

Abstract

Mitigating cracking distress in asphalt concrete is a major challenge for road agencies around the world and assessment of fracture and crack propagation in asphalt concrete has proven an equally difficult task. Many of the current fracture mechanics based tests available to assess asphalt concrete are based on the assumption of elastic behavior and it is difficult to extend the analysis to assess fracture at intermediate pavement service temperatures. In addition, the difficulty of monitoring crack length and propagation has led to asphalt concrete related test methods that focus solely on fracture mechanics parameters with little regard for crack speed. The C* Line Integral test was identified as a promising test to evaluate crack propagation and obtain the fracture mechanics based, C* parameter that considers time-dependent creep behavior of the materials. The test is not well defined in previous literature and lacks a test procedure and detailed data analysis method. This paper describes test method development of a notched disk crack propagation test for asphalt concrete, the C* Fracture Test (CFT). Development included specimen geometry, test temperature variation study, and a refined data analysis procedure. Two distinct plant produced asphalt mixtures were also subjected to the crack propagation test and results indicated that the CFT was able to distinguish improved crack resistance potential of an asphalt-rubber mixture compared to an unmodified asphalt mixture. The asphalt-rubber mixture was more resistant to crack propagation than the unmodified mixture. Continuous monitoring of the field test sections is necessary to validate the laboratory findings.

Keywords: Asphalt concrete; Fracture; Crack growth; Fracture mechanics; Propagation

Review Article

Volume 3 Issue 5 - 2017

Jeffrey Stempihar¹ and Kamil E Kaloush^{2*}

¹Assistant Research Professor, Arizona State University, USA

²Professor, Arizona State University, USA

***Corresponding author:** Kamil E Kaloush, Professor, Arizona State University, Tempe, AZ, USA, Email: Kamil.Kaloush@asu.edu

Received: November 20, 2017 | **Published:** December 07, 2017

Background

Cracking is a major distress in asphalt pavement which can lead to premature pavement failures and can cost agencies millions of dollars in maintenance and rehabilitation costs. Even with modern advances in pavement engineering, attempts to quantify and model cracking in asphalt pavements have proved extremely challenging; this is due to the visco-elastic behavior of asphalt concrete and the complex stress states that exist in pavement layers due to loading or thermally induced stresses. Since its introduction to asphalt concrete by Majidzadeh [1] fracture mechanics has been used to characterize cracking in flexible pavement design and laboratory evaluation of crack resistance of asphalt concrete. Several tests have either been developed or adopted from other fields to evaluate asphalt concrete fracture in the laboratory. The more common laboratory fracture tests include the indirect tension test (IDT) [2], semi-circular bend test (SCB) [3], direct compact tension test (DCT) [4], Fénix test [5], single edge notched beam (SEB) [6,7], and the Texas Overlay Tester (OT) as shown in Figure 1. Linear elastic fracture mechanics (LEFM) parameters that can be calculated from data obtained from these tests include: stress intensity factor (K) and fracture energy (G), which require the assumption of linear elastic material behavior [8]. The J parameter can also be obtained from certain tests and assumes elastic-plastic behavior. Although the aforementioned

tests deserve great merit and consideration, a standard test or a single parameter has not been fully developed that can provide reliable fracture properties of asphalt concrete [4]. More recently Walubita et al. [9] conducted a study to compare four cracking test methods in order to investigate methods to screen and select crack resistant HMA mixes which can potentially mitigate fatigue cracking. The four laboratory tests included the overlay tester (OT), direct tension (DT), indirect tension (IDT), and semicircular bending (SCB). Authors used an evaluation criteria based on: test rationality, comparison to field performance; repeatability, variability and practicality, ease of specimen fabrication, and effort required for data analysis. Authors determined that the DT, IDT and SCB tests produced more repeatable results, however; they could not properly distinguish crack resistance based on tensile strength and strain parameters. The OT test produced less repeatable results than the other tests included in the study. Authors concluded that none of the tests considered would be recommended as a simple laboratory test to assess fatigue. The study recommended further evaluation of the IDT and SCB tests using repeated loading and comparison to field performance. Of the two, the IDT was recommended as the primary choice for further analysis. The C* Line Integral has been used to a limited extent in asphalt concrete cracking evaluation and was identified as a promising test method [10]. The test provides a fracture mechanics parameter (C*) and also the crack growth

rate (a^*). The C^* parameter obtained from this test considers the time-dependent behavior of asphalt and can be converted to the stress intensity factor (K) when elastic behavior of asphalt concrete prevails at low temperatures. This alone makes the C^* a very universal parameter to describe crack resistance behavior of asphalt concrete. Since its application to asphalt mixtures by Abdulshafi [11], the C^* Line Integral has been used to successfully rank crack resistance of asphalt pavements with modified and unmodified asphalt [11-13]. However, further research efforts were identified and needed to develop a standard test procedure, refined data analysis procedure and further evaluate the ability of the modified test method to capture differences in crack propagation rates in plant produced mixtures.

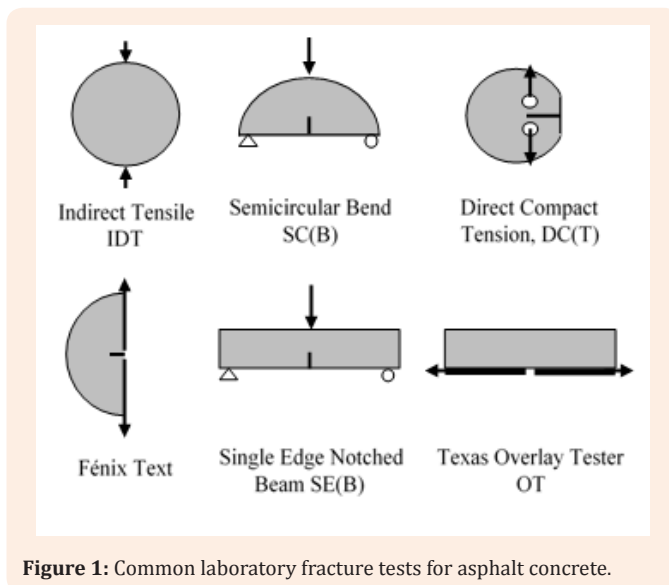


Figure 1: Common laboratory fracture tests for asphalt concrete.

C^* Parameter

The C^* parameter was first applied to fracture mechanics by Landes & Begley [14] to describe the stresses and strains surrounding the crack tip region in metals at high temperatures. C^* can be described as an energy rate line integral that describes the stress and strain rate field surrounding the crack tip in a viscous material. This parameter was developed based on the J-integral which describes the crack tip conditions in elastic or elastic-plastic materials [14-16]. However, the C^* parameter can provide a more general case for materials which exhibit brittle and creep fracture [17]. For stationary steady-state creep conditions, C^* is a parameter which relates the creep power dissipation rate to crack propagation [15]. It is important to note that this parameter assumes a nonlinear and steady-state creep law, which means that C^* is only applicable to long-term behavior. Also, authors note that C^* is not applicable to characterize creep crack growth in all ranges of cracking behavior. Experimental measurement of C^* can be accomplished due to the relationship between the J-integral and C^* parameter. J is defined as the energy difference between two specimens that have varying crack lengths for the same applied load. In comparison, C^* can be calculated as power

or energy rate difference between two specimens, loaded the same, with incrementally differing crack lengths [14]. Given two identical specimens with different crack lengths, C^* is a measure of the change in power necessary to propagate each crack a distance of " dl " within the material. Mathematically, C^* can be expressed by Equation 1. Since potential energy is a function of crack length, load and displacement, the partial derivative must be taken for a fixed load (P) and displacement (\hat{u}). The potential energy can be found as the area under the load-displacement rate curve for any given specimen [14]. Equation 1 presents the calculation of the C^* parameter [11].

$$C^* = \left(-\frac{1}{b} * \frac{dU^*}{dl} \right)_{P, \hat{u}} \quad (1)$$

Where:

U^* = power or energy rate for a given load, P and displacement \hat{u} , given by:

$$U^* = \int_0^{\hat{u}} P d\hat{u} \quad (2)$$

b = specimen thickness.

Experimental evaluation of the C^* method can be accomplished using the graphical method proposed by Landes & Beagley [14] and summarized in the following steps which are shown graphically in Figure 2.

- For static loading, plot load (P) and crack length (a) as a function of time.
- Use Step 1 data to plot load divided by specimen thickness (P/t) versus displacement rate (Δ^*) for each incremental crack length (a). The area under each $P-\Delta^*$ curve per incremental crack length represents the power or energy rate (U^*).
- Plot U^* versus crack length for each displacement rate. C^* is taken as the slope of a linear fit of these data.
- Plot C^* and a^* versus displacement rate, and
- Plot the crack growth rate (a^*) as a function of C^* on a log-log plot.

Research objective

The main objective of this paper is to present the development of the C^* Fracture Test (CFT) for asphalt concrete based on improvements to the original C^* Line Integral test. This objective was achieved by establishing and documenting a test methodology for the CFT, conducting tests on a laboratory prepared mixture at 21°C to recommend a test specimen size, evaluating the ability of the CFT to capture temperature effects, detailing the data analysis procedure and test conditions, and evaluating two distinct plant produced asphalt mixtures [18].

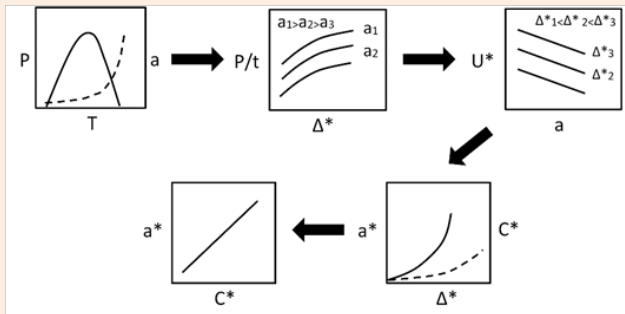


Figure 2: Graphical steps to determine C^* parameter [14].

C^* Fracture test setup

The CFT apparatus was based partially on the setup developed by Abdulshafi [11] and modified by Kaloush et al. [13]. Two stainless steel loading plates (3 mm thick) with right-angled edges were used to form the loading plates placed in the right angle, notched cut. A Lottman Breaking Head was modified at the Arizona State University (ASU) machine shop to produce a loading head with appropriate radius such that a point load is applied at a distance halfway along each notch face. Figure 3 presents a schematic of the CFT apparatus and photo of an actual specimen loaded into the apparatus. Frictionless lubricant was applied to the faces of the plates which contact the loading head. The dimensions of the modified loading head which mounts to the top plate of the Lottman Breaking Head are presented in Figure 4.

Specimen preparation

Different specimen geometry was evaluated as part of this study, but the specimen preparation method will be described using a 150 mm diameter by 50 mm thick specimen as an example. CFT specimens were produced by cutting two 50 mm thick specimens from the center of a 150 mm diameter by 170 mm tall gyratory compacted sample. A right-angle notch (25 mm deep) was carefully cut into the specimen using a water-cooled diamond blade and a jig to hold the specimen. The specimen was rotated 45° in each direction from the vertical centerline to facilitate cutting the notch edges vertically. Next, a diamond coated scroll saw blade was used to introduce a 3 mm deep by 1.6 mm wide initial crack into the specimen. Finally, the specimen face was painted white

using acrylic paint and 10 mm incremental lines were marked on the specimen face to monitor crack progression during the test. Figure 5 presents the sequence of specimen preparation. For the case of the 100 mm diameter specimens described in a later section, 100 mm cores were taken from the center of a 150 mm diameter by 170 mm tall gyratory compacted sample. The right angle notch was cut to a depth of 19 mm and a 3 mm deep by 1.6 mm wide initial crack was introduced into the specimen. Testing was conducted using a servo-hydraulic, Universal Testing Machine with 100 kN load capacity and environmental control chamber. Crack propagation rate was captured using a high definition digital video camera and crack length versus time measurements were extracted visually from video playback. Figure 6 presents an example of a cracked specimen at the completion of a test.

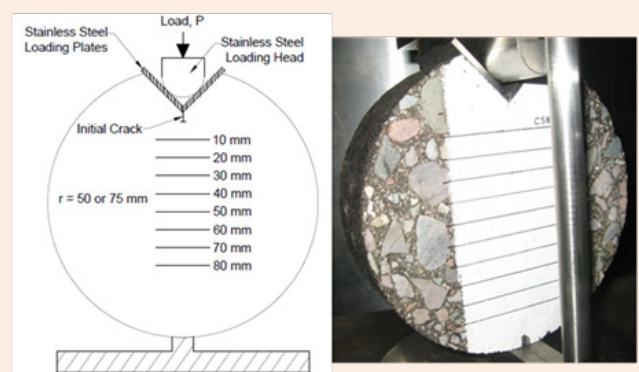


Figure 3: C^* Fracture Test setup.

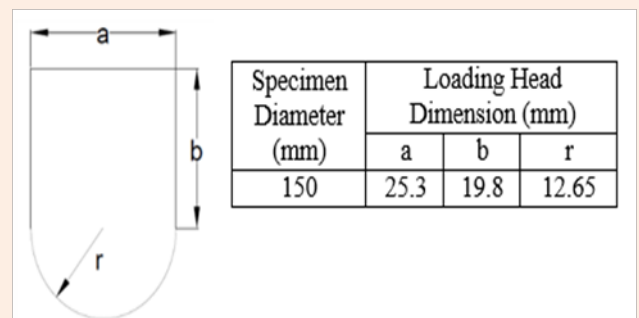


Figure 4: CFT loading head dimensions.

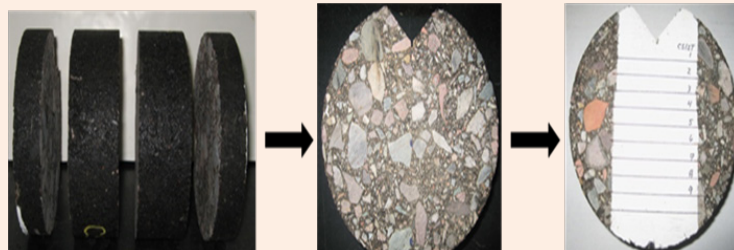


Figure 5: Specimen preparation sequence.



Figure 6: Example of crack specimen at the completion of CFT.

Material properties

Asphalt concrete samples used for testing in this part of the study were laboratory prepared using local Arizona materials and asphalt binder. The asphalt mixture consisted of a dense-graded, Arizona Department of Transportation (ADOT) mixture using a nominal maximum aggregate size of 19 mm. PG70-10 binder was used at a rate of 4.6% by total weight of mixture. Maximum theoretical specific gravity (G_{mm}) of the mixture was determined in the laboratory as 2.482 and the target laboratory air voids were $6.0 \pm 0.6\%$. The gradation, presented in Table 1, was created using Salt River aggregates obtained from the CEMEX Inc. asphalt plant located in the greater Phoenix, Arizona area. Specimen Geometry Study. The experimental plan to investigate specimen geometry and test temperature was developed considering test temperatures and specimen sizes commonly used in laboratory testing of asphalt concrete. The factors considered included: specimen diameter and thickness. The intent was to recommend a specimen size for the CFT procedure prior to investigating any temperature effects. Three specimen sizes were considered (diameter x thickness): 150 x 50 mm, 150 x 25 mm and 100 x 50 mm and all tests were

carried out at 21°C. Specimens with these dimensions can easily be obtained from Marshall or gyratory compaction equipment. For each geometric configuration, 10 specimens were tested; two replicates at each of the following displacement rates: 0.15, 0.228, 0.30, 0.378 and 0.45 mm/min which were based on ranges found in literature [11-13]. The average air voids for the 150 x 50 mm, 150 x 25 mm, and 100 x 50 mm specimen sizes were 6.04 %, 5.95 % and 5.97 %, respectively. Table 2 provides a summary of all C^* and a^* data from the geometric study. Crack growth rates and C^* values increase with increasing displacement rate which is expected. Figure 7 presents the a^* - C^* trends graphically and from the results, it is evident that a^* - C^* trends from 150 x 25 mm specimens are different than trends from 150 x 50 mm and 100 x 50 mm specimens. Also, it appears that 150 x 50 mm and 100 x 50 mm specimens produce similar a^* - C^* for the test conditions. Thus, from these results specimen thickness plays a more significant role in the C^* and crack growth rate data than specimen diameter.

Table 1: Aggregate gradation.

Sieve Size (mm)	% Passing
25	100
19	91
12.5	83
9.375	76
4.75	60
2.36	46
1.18	32
0.6	22
0.3	13
0.15	8
0.075	4.9

Table 2: CFT results at 21°C.

Diameter (Thickness)	Displacement Rate (mm/min)	Average Crack Growth Rate (m/hr)	Crack Growth Rate C.V. (%)	Average C^* MJ/m ² -hr	C^* C.V. (%)
150 mm (50mm)	0.15	1.13	0.7	1.03E-02	8.2
	0.228	1.54	25.6	1.79E-02	6.9
	0.3	2.37	14.9	2.47E-02	7.2
	0.378	3.23	46.7	3.29E-02	7.7
	0.45	4.22	5	4.24E-02	6.1
150 mm (25mm)	0.15	1.22	18.5	1.07E-02	14.4
	0.228	1.44	32.1	1.73E-02	17.8
	0.3	3.15	19.5	2.33E-02	20.4
	0.378	5.31	12.6	3.03E-02	18.3
	0.45	5.14	14.3	3.75E-02	15.6
100 mm (50mm)	0.15	0.9	34.7	1.22E-02	24.2
	0.228	1.91	21.5	1.98E-02	20.8
	0.3	2.98	3.7	2.71E-02	15.1
	0.378	3.26	21.2	3.52E-02	9.8
	0.45	3	14.5	4.31E-02	7.1

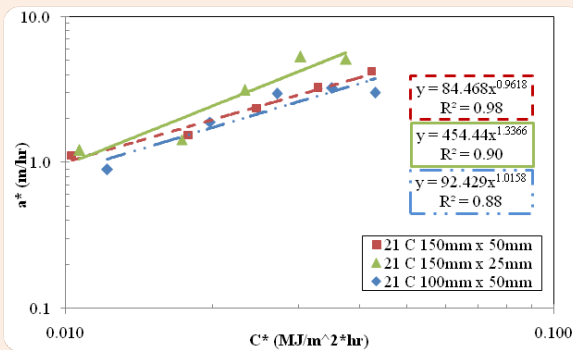


Figure 7: Effect of specimen size on CFT results at 21°C.

Statistical comparison

Statistical comparison was performed in order to determine if the crack growth rate versus C^* trends (Figure 7) obtained from different size specimens produced statistically different trends. A log transformation was required in order to use linear regression techniques and the assumption of equal variance and normality was verified. Two regression equations were compared by fitting Equation (1) to the combined data. An indicator variable was required in this analysis in order to distinguish between the trends obtained from the two different specimen sizes being compared [19].

$$\log a^* - \alpha + \beta \log C^* + \gamma \text{Size} + \delta \log C^* * \text{Size} \quad (3)$$

Where:

a^* = crack growth rate (m/hr),

C^* = power release rate parameter (MJ/m²-hr),

Size = indicator variable (0 or 1) to distinguish specimen sizes, and

$\alpha, \beta, \gamma, \delta$ = regression parameters.

The hypothesis test for the comparison was as follows and statistical analysis was performed using level of significance of 0.05:

H_0 : Both γ and $\delta = 0$

H_a : Not both γ and $\delta = 0$

Accepting the null hypothesis (H_0) indicated that specimen size was statistically insignificant and a^* - C^* regression trends produced from different size CFT specimens were not statistically different. In comparison, rejection of the null hypothesis indicated that specimen size has an impact on a^* - C^* regression trends and should not be disregarded. Statistical software was used for all statistical analyses. Table 3 presents the results of the statistical analysis for a 0.05 level of significance. If the p-value is less than the level of significance, the null hypothesis (H_0) is rejected. At a level of significance of 0.05, there is a statistical difference between a^* - C^* trends obtained in the CFT using 150 x 25 mm and 100 x 50 mm specimen sizes. The " γ " parameter is significant indicating

the y-intercept values are statistically different between the two trends and the combined dataset cannot be represented by a single regression function. These results are in line with practical consideration of a^* - C^* trends presented in Figure 7 except for the comparison between 150 x 50 mm and 150 x 25 mm specimen sizes. Visual comparison of these data indicates a physical difference in the trends; crack propagation rates are more rapid in the 150 x 25 mm specimens compared to the 150 x 50 mm specimens for the range of C^* values obtained from the test.

Table 3: Statistical analysis results considering specimen size.

Comparison (Size, mm)	Parameter	p-Value	$\alpha = 0.05$ Decision
150 x 50 vs. 150 x 25	γ	0.08	Accept H_0
	δ	0.2	Accept H_0
150 x 50 vs. 100 x 50	γ	0.34	Accept H_0
	δ	0.82	Accept H_0
150 x 25 vs. 100 x 50	γ	0.04	Reject H_0
	δ	0.38	Accept H_0

Recommended specimen geometry

Based on the results of the specimen geometry study the recommended test geometry is a specimen of 150 mm diameter and 50 mm thickness. The right angle notch length shall be 25 mm and an initial crack of 3 mm deep by 1.6 mm wide shall be cut at the bottom of the notch. The following provides support for selection of the recommended specimen size.

1. 150 mm diameter specimen can easily be obtained from the Superpave gyratory compactor or field cored specimens,
2. Specimen diameter of 150 mm produces a dimension of four times the nominal maximum aggregate size for typical Superpave mixtures.
3. Specimen thickness of 50 mm provides a dimension of four times the 12.5 nominal maximum aggregate for typical Superpave surface course mixtures.
4. Specimen diameter of 150 mm provides a large surface area for crack propagation.
5. Data analysis indicated that 150 x 50 mm specimens produced the best statistical fit of a^* - C^* data trends (highest R^2 -values).

While statistical analysis and physical observation of test results presented in Figure 7 indicate no difference between a^* - C^* trends obtained from 150 x 50 mm and 100 x 50 mm specimens, the 150 mm diameter specimen is preferred for the aforementioned reasons.

Effect of temperature test results

In an effort to determine if the CFT can capture a temperature effect on crack propagation rates within an intermediate pavement temperature range, additional specimens were tested at 4.4°C and 10°C to supplement the previous results at 21°C. All tests were

conducted using the recommended specimen size of 150 mm x 50 mm and results are presented in Table 4. The average air voids for specimens tested at 4.4°C, 10°C, and 21°C were 5.87 %, 5.79 % and 6.04 %, respectively. Figure 8 shows the crack growth rate trends graphically for all test temperatures. These results are rational in that for a given C^* -value, crack growth rate increase with decreasing temperature or the C^* trends shift to the left with decreasing temperature. For example, a C^* value of 0.02 MJ/m²-hr would yield crack propagation rates of 30.9, 6.2, and 2.0 m/hr at 4.4°C, 10°C and 21°C, respectively. C^* Fracture Tests were carried out on the control and rubber modified mixtures using UTM-100 test equipment at 4.4°C and test data are presented in Table 6. Crack growth rate is plotted as a function of C^* for each

mixture and is presented in Figure 9 and modeled using a power function. From these laboratory test data, the PG64-22AR mixture exhibits better resistance to crack propagation compared to the PG76-22 unmodified mixture at 4.4°C. For a C^* value of 0.05 MJ/m²-hr, the crack propagation rates are 5.0 m/hr and 1.1 m/hr for the unmodified and asphalt-rubber mixtures, respectively. Test results provide substantiation that the CFT can effectively be conducted in the temperature range of 4.4°C to 21°C and crack growth rates can be captured with excellent statistical measures of fit. It is anticipated that the CFT can be effective at capturing crack growth in the intermediate pavement temperature range, however additional mixture types must be tested to validate this finding.

Table 4: CFT results at 4.4, 10, and 21°C.

Test Temperature (°C)	Displacement Rate (mm/min)	Average Crack Growth Rate (m/hr)	Crack Growth Rate C.V. (%)	Average C^* MJ/m ² -hr	C^* C.V. (%)
4.4	0.03	2.11	51.5	2.72E-03	13.9
	0.06	6.57	29.8	6.24E-03	4.8
	0.102	16.69	21	1.14E-02	3
	0.15	35.81	1.71	1.80E-02	5.3
10	0.072	1.98	6.6	7.31E-03	19.3
	0.15	4.68	22.4	1.78E-02	20.4
	0.228	9.68	58.6	2.81E-02	8.7
	0.3	12.48	8.6	3.55E-02	7.3
21	0.15	1.13	0.7	1.03E-02	8.2
	0.228	1.54	25.6	1.79E-02	6.9
	0.3	2.37	14.9	2.47E-02	7.2
	0.378	3.23	46.7	3.29E-02	7.7
	0.45	4.22	5	4.24E-02	6.1

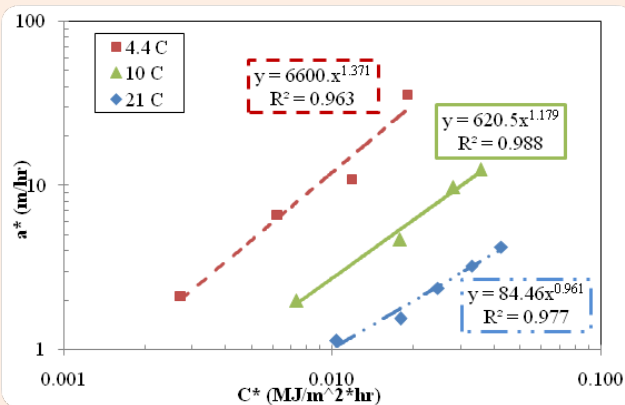


Figure 8: Effect of temperature on CFT results.

Recommended data analysis procedure

Based on the results of the specimen size and temperature effect study, the following provided recommendations to refine

the recommended data analysis procedures to calculate the C^* parameter and crack growth rate from the C^* Fracture Test. Detailed explanation on the development of these recommendations is presented by Stempihar [18].

- Step 1:** For static loading, plot load (P) and crack length (a) as a function of time. Calculate the crack growth rate using a linear fit of crack length versus time data between 20-80 mm crack lengths.
- Step 2:** Use Step 1 data to plot normalized load (by specimen thickness) (P/t) versus displacement rate (Δ^*) for each incremental crack length (a) between 20-80 mm. The area under each P - Δ^* curve per incremental crack length represents the power or energy rate (U^*). Determine the area utilizing the average end area method. The first area increment, between zero and the initial displacement rate, shall be calculated by multiplying the initial displacement rate by a factor of 0.8 and then by the corresponding P/t value.
- Step 3:** Plot U^* as a function of crack length for each displacement rate between 20-80 mm crack length

intervals. The C^* -parameter is taken as the slope a linear fit of these data.

4. **Step 4:** Plot C^* and a^* as a function of displacement rate (Δ^*) and model using a power relationship to access the quality of the data.
5. **Step 5:** Plot crack growth rate (a^*) versus C^* on a log-log plot and use a power model to represent the data.

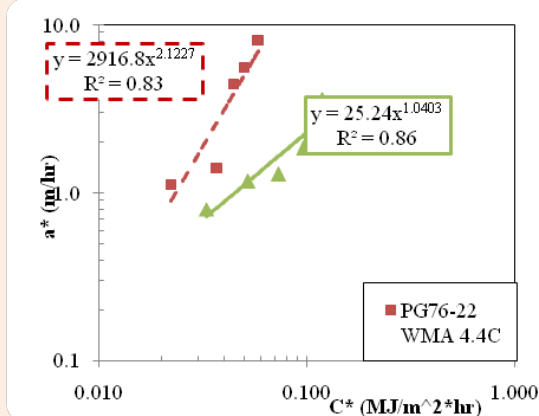


Figure 9: a^* - C^* relationship for I-78 mixtures.

Plant produced mixture evaluation

The final objective in this research study was to evaluate two plant produced mixtures using the CFT to assess the ability of the laboratory test to distinguish between an unmodified and asphalt-rubber modified mixture. Samples of two mixtures, constructed on I-78 in Pennsylvania in 2012 were tested using the C^* Fracture Test. These I-78 mixtures consisted of two warm-mix asphalt mixtures designed for >30 million ESALs; a 9.5mm unmodified section (PG76-22) and a 12.5 mm, gap-graded, asphalt-rubber (PG64-22 AR) section. This was the first use of a gap-graded, wet process asphalt rubber mixture in the state and this section was being compared to the typical surface course mixture used in the region. The unmodified mixture targeted 5.7% of PG76-22 whereas the asphalt-rubber mixture targeted 8.1% of PG64-22 binder and contained 18% crumb rubber by weight of binder. Binders for both mixtures were blended with 0.5% Evotherm. Maximum theoretical specific gravity measured in the laboratory was 2.498 and 2.407 for the unmodified and asphalt-rubber mixtures, respectively and a target air void level of $6.5 \pm 0.65\%$ was set for all specimens produced and tested in the laboratory. Table 5 presents the gradation used for both mixtures. C^* Fracture Tests were carried out on the control and rubber modified mixtures using UTM-100 test equipment at 4.4°C and test data are presented in Table 6. Crack growth rate is plotted as a function of C^* for each mixture and is presented in Figure 9 and modeled using a power function. From these laboratory test data, the PG64-22AR mixture exhibits better resistance to crack propagation compared to the PG76-22 unmodified mixture at 4.4°C. For a C^* value of 0.05 MJ/m²-hr, the crack propagation rates are 5.0 m/hr and 1.1 m/hr for the unmodified and asphalt-

rubber mixtures, respectively. CFT results from the I-78 mixtures, tested at 4.4°C, indicate that the test is able to capture differences in crack propagation between an unmodified and asphalt-rubber mixture. The lower statistical measures of fit (R^2) compared to the laboratory prepared specimens test results are the expected inherent variation in mixture homogeneity due to sampling techniques. Field distress survey data, collected in 2015, were provided by the Pennsylvania Department of Transportation to assess the level of cracking. After three years of service life, the unmodified and asphalt-rubber modified mixtures exhibited similar low and medium severity transverse cracking distress levels. It is expected that the performance trends of these mixtures will match CFT test results with increased service life and continuous monitoring of the field test sections is necessary.

Table 5: I-78 mixture gradations.

Sieve Size (mm)	% Passing	
	9.5 mm Wearing	12.5 mm Gap (18% Crumb Rubber)
19	100	100
12.5	100	97
9.5	95	84
4.75	59	30
2.36	45	22
1.18	27	14
0.6	17	9
0.3	12	7
0.15	8	6
0.075	5.5	5

C^* Fracture test recommendations

Based on C^* Fracture Test results from laboratory and field mixtures, the following recommendations are presented:

1. Recommended specimen geometry is 150 mm in diameter by 50 mm thick with a 25 mm deep right angle notch and 3 mm deep, mechanically introduced initial crack.
2. Tests shall be conducted in the range of 4.4 - 10°C.
3. Recommendations for initial displacement rates are 0.15 and 0.30 mm/min at test temperatures of 4.4 and 10°C, respectively.
4. Data analysis method has been refined and clarified as described herein.
5. For each mixture, testing should be carried out at four loading rates with two replicates at each rate. However, if mixture quantity is limited, a minimum of five loading rates shall be tested using one replicate [18].

Table 6: C* and crack growth data for I-78 mixtures.

Temp. (°C)	Mixture	Displacement Rate (mm/min)	Crack Growth Rate (m/hr)	C* MJ/m ² ·hr
4.4	PG76-22 WMA	0.15	1.13	2.21E-02
		0.228	1.41	3.71E-02
		0.264	4.46	4.42E-02
		0.3	5.62	4.98E-02
		0.378	8.17	5.86E-02
	PG64-22 AR WMA	0.3	0.81	3.28E-02
		0.45	1.18	5.22E-02
		0.6	1.3	7.30E-02
		0.75	1.86	9.54E-02
		0.9	3.62	1.18E-01

Conclusion

A notched disk crack propagation test, the C* Fracture Test (CFT), presented in this paper is a promising test to assess crack propagation and fracture resistance of asphalt concrete mixtures. An improved CFT test procedure was developed based on a laboratory study of different specimen geometries and test temperatures. A 150 x 50 mm notched disk test specimen is proposed as the standard size based on a laboratory study using a laboratory produced mixture at 21°C. This size specimen can easily be produced from a gyratory compactor and also provides ample area for crack growth and monitoring. Using this specimen size, additional tests were carried out at 4.4°C and 10°C to evaluate the effect of test temperature on CFT results for the same laboratory produced mixture. These temperatures were selected to represent intermediate pavement temperatures where creep related crack propagation is likely to occur. The CFT yielded reasonable crack growth rate trends in the temperature range between 4.4°C and 21°C. CFT results from two plant produced mixtures constructed on I-78 in Pennsylvania, tested at 4.4°C, indicate that the CFT is able to capture differences in crack growth rates between unmodified and asphalt-rubber modified mixtures. CFT results indicated that the asphalt-rubber mixture was more resistant to crack propagation than the unmodified mixture which matches expected field performance of an asphalt-rubber mixture evaluated in terms of resistance to cracking. Field distress survey data, collected in 2015, were provided by the Pennsylvania Department of Transportation to assess the level of cracking. After three years of service life, the unmodified and asphalt-rubber modified mixtures exhibited similar levels of low and medium severity transverse cracking distress levels. It is expected that the performance trends of these mixtures will match CFT test results with increased service life and continuous monitoring of the field test sections is necessary. Finally, a recommended data analysis method was presented along with recommended test conditions. Based in the findings presented herein, the C* Fracture Test can be a viable laboratory test to describe crack propagation in asphalt concrete.

Recommendations

Conclusions are based on limited mixture testing and volumetric properties and thus; additional mixtures should be analyzed using the CFT to confirm and supplement research findings. Field and laboratory mixtures, subjected to the test should vary by gradation, binder type and content, air-voids and mixture modification. Data should be used to confirm or expand findings and refine recommended test conditions.

Acknowledgement

None.

Conflict of Interest

None.

References

1. Majidzadeh K, EM Kauffmann, DV Ramsamooj, Chan AT (1970) Analysis of Fatigue and Fracture of Bituminous Paving Mixtures, Report No. 2546. US Bureau of Public Roads. Research and Development, USA
2. Christensen DW, Bonaquist RF (2004) NCHRP Report 530: Evaluation of Indirect Tensile Test (IDT) Procedures for Low-Temperature Performance of Hot Mix Asphalt. Transportation Research Board-National Research Council, Washington, DC National Academy Press, USA.
3. Krans RL, Tolman F, Van de Ven MFC (1996) Semi-Circular Bending Test: A Practical Crack Growth Test using Asphalt Concrete Cores. Reflective Cracking in Pavements, RILEM, London: E & FN Spon 123-132.
4. Wagoner MP, Buttlar W, Paulino G (2005) Disk-Shaped Compact Tension Test for Asphalt Concrete Fracture. Society for Experimental Mechanics 45(3): 270-277.
5. Pérez-Jiménez F, Valdés G, Miró R, Marínez A, Botella R (2010) Fénix Test Development of a New Test Procedure for Evaluating Cracking Resistance in Bituminous Materials. Transportation Research Record 2181: 36-43.

6. Lee NK, Hesp SAM (1994) Low Temperature Fracture Toughness of Polyethylene-Modified Asphalt Binders, Transportation Research Record 1436: 54-59.
7. Lee NK, Morrison GR, Hesp SAM (1995) Low Temperature Fracture Toughness of Polyethylene-Modified Asphalt Binders and Asphalt Concrete Mixes. Journal of the Association of Asphalt Paving Technologists 64: 534-574.
8. Germann FP, Lytton RL (1979) Methodology for Predicting the Reflection Cracking Life of Asphalt Concrete Overlays, Research report.
9. Walubita L, Jamison B, Das G, Scullion T, Martin AE, et al. (2011) HMA Crack Characterization: Search for Laboratory Test to Evaluate HMA Mixture Crack Resistance. Transportation Research Record 2210: 73-80.
10. Vinson TS, Janoo V, Haas R (1989) SHRP-A-306 - Low Temperature and Thermal Fatigue Cracking SR-OSU-A-003A-89-1. Transportation Research Board, Washington DC, USA,
11. Abdulshafi O (1983) Rational Material Characterization of Asphaltic Concrete Pavements, Ph.D. Dissertation, The Ohio State University, USA.
12. Abdulshafi A, Kaloush K (1988) Modifiers for Asphalt Concrete, ESL-TR-88-29. Air Force Engineering and Technical Services Center, Tyndall Air Force Base, Florida, USA.
13. Kaloush K, Biligiri K, Zeiada W, Rodezno M, Reed, J (2010) Evaluation of Fiber-Reinforced Asphalt Mixtures Using Advanced Material Characterization Tests. ASTM Journal of Testing and Evaluation 38(4): 1-12.
14. Landes JD, Begley J (1976) A Fracture Mechanics Approach to Creep Crack Growth. Mechanics of Crack Growth, Proceedings of the Eighth National Symposium on Fracture Mechanics 590: 128-148.
15. Wu D, Christian EM, Ellison EG (1984) Evaluation of Creep Crack C* Integrals. Journal of Strain Analysis 19 (3):185-195.
16. Anderson TL (2005) Fracture Mechanics 3rd Edition, Fundamentals and Applications.
17. Abdulshafi O (1992) Effect of Aggregate on Asphalt Mixture Cracking Using Time-Dependent Fracture Mechanics Approach. Effects of aggregate and Mineral Fillers on Asphalt Mixture Performance, ASTM STP1147-EB, American Society for Testing and Materials, Philadelphia, USA.
18. Stempihar, Jeffrey J (2013) Development of the C* Fracture Test for Asphalt Concrete Mixtures. Dissertation, Arizona State University, USA.
19. Neter J, Kutner M, Nachtsheim C, Wasserman W (1996) Applied Linear Regression, Third Edition. Chicago: IRWIN, USA.